Organic molecular films on gold versus conducting polymer: Influence of injection barrier height and morphology on current–voltage characteristics

N. Koch[a)]
Department of Electrical Engineering and Department of Chemistry, Princeton University, Princeton, New Jersey 08544

A. Elschner
H.C. Starck GmbH, c/o Bayer AG Uerdingen, D-47829 Krefeld, Germany

J. Schwartz
Department of Chemistry, Princeton University, Princeton, New Jersey 08544

A. Kahn[b)]
Department of Electrical Engineering, Princeton University, Princeton, New Jersey 08544

(Received 27 November 2002; accepted 7 February 2003)

The current–voltage characteristics $I(V)$ of model organic devices are studied under ultra-high-vacuum conditions. Active materials are N,N′-bis-(1-naphthyl)-N,N′-diphenyl1-1,1-biphenyl1-4,4′-diamine (α-NPD) and pentacene, electrode materials are polycrystalline Au and the conductive polymer poly(3,4-ethylenedioxythiophene)/poly(styrenesulfonate) (PEDOT/PSS). Despite a similar work function of electrode material surfaces ($\sim$5 eV), hole injection from PEDOT/PSS is significantly more efficient than from Au, due to a smaller hole injection barrier. Hole injection characteristics from Au electrodes for devices made from α-NPD are independent of deposition sequence and substrate used. Pentacene devices exhibit serious asymmetries in that respect. These are caused by a strong dependence of morphology and preferred molecular orientation on the substrate for the crystalline material. © *2003 American Institute of Physics.* [DOI: 10.1063/1.1565506]

The performance of organic-based electronic and optoelectronic devices depends in a very direct way on the electronic structure of metal/organic interfaces and the charge carrier injection efficiency at these interfaces. Up to a few years ago, a widespread misconception was the assumption of a linear relationship between the work function of the electrode material and the charge injection barrier to the organic material. From 1997 on, a considerable amount of work done by several groups[1–4] started to dispel this notion by demonstrating the existence of large dipole barriers at metal/organic interfaces. The origin of these dipoles has since been traced to various mechanisms, such as charge transfer with[5] and without[2] interface chemistry, or modification of the metal substrate work function by the organic molecules.[1,6] Recently, photoemission experiments on interfaces formed between the hole transport material N,N′-bis-(1-naphthyl)-N,N′-dphenyl1-1,1-biphenyl1-4,4′-diamine (α-NPD) and pentacene and two large work function anode materials, gold and the conductive polymer poly(3,4-ethylenedioxythiophene)/poly(styrene sulfonate) (PEDOT/PSS),[7,8] have shown that the magnitude of the interface dipole may depend in a substantial way on the physical nature of the anode material, i.e., metal versus conducting polymer, rather than on its work function alone.[9] In Ref. 9, we demonstrate that the hole injection barriers from Au into α-NPD and pentacene are 1.4 and 0.85 eV, respectively, whereas these barriers are reduced to 0.4 and 0.25 eV when PEDOT/PSS is used, despite the nearly identical work functions of the two electrode material surfaces ($\sim$5 eV). The principal reason behind this difference is believed to be the way in which the organic molecules deposited on the metallic substrate modify the work function of that substrate. The work function of Au has a strong surface electronic component corresponding to electrons tailing into the vacuum. The compression of this tail by deposited molecules leads to an abrupt decrease of the work function and to the interface dipole, or vacuum level shift ($\sim$0.5–1 eV) between the two materials. The work function of the conducting polymer, on the other hand, does not have such a large surface electronic component, and the deposition of organic molecules introduces only a modest dipole between the two materials. Note that a charge transfer reaction between PSS and the deposited organic material cannot be entirely ruled out at this point.

An important aspect of the work on interfaces is the verification that the electronic structure derived from surface/interface spectroscopy actually translates into device behavior. In this letter, we demonstrate that the lowering of the hole injection barriers when PEDOT/PSS is used instead of Au is directly manifested in current–voltage characteristics $I(V)$ of hole-only devices comprised of the molecular organic materials and Au or PEDOT/PSS electrodes. While $I(V)$ data obtained for amorphous films of α-NPD on both types of substrate, Au and the polymer, are consistent with

[a)]Present address: Humboldt-Universiät zu Berlin, Institut für Physik, Invalidenstrasse 110, D-10115 Berlin, Germany.
[b)]Author to whom correspondence should be addressed; electronic mail: kahn@ee.princeton.edu

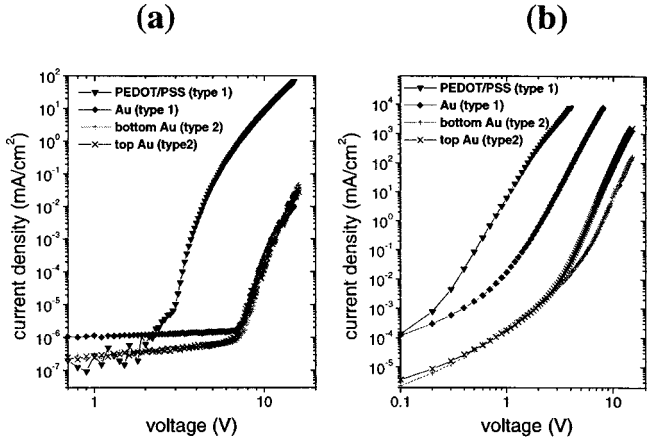

FIG. 1. $I(V)$ curves for ITO/(PEDOT/PSS)/organic(150 nm)/Au(45 nm) (type 1) devices, and ITO/(PEDOT/PSS)/Au(80 nm)/organic(150 nm)/Au(45 nm) (type 2) devices: (a) α-NPD; (b) pentacene.

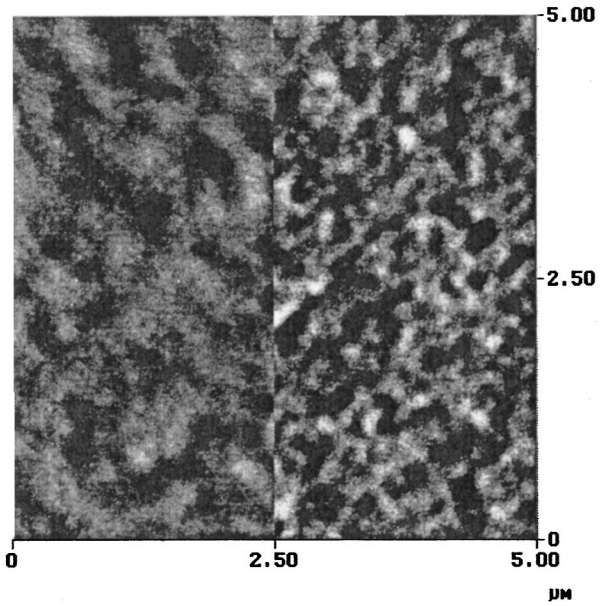

FIG. 2. AFM micrograph of 150-nm-thick α-NPD films on PEDOT/PSS (left half) and on Au (right half). The height scale is 10 nm.

expectations, data for crystalline pentacene on the two substrates films exhibit significant divergence. An atomic force microscopy (AFM) study of the organic films reveals pronounced differences in film morphology and molecular preferred orientation, which accounts for the observed variations in $I(V)$ curves.

PEDOT/PSS (Baytron P AI 4083, H.C. Starck) was spin cast from aqueous solution onto commercial ITO covered glass slides (Merck) following standard procedures. After annealing (120 °C) in air these substrates were loaded into a custom-made multichamber ultra-high-vacuum system (base pressure lower than 2×10^{-8} mbar during experiments with PEDOT/PSS electrodes, and lower than 2×10^{-9} mbar during experiments with Au electrodes) for device fabrication and analysis. α-NPD and pentacene (both from Aldrich Co.) were evaporated from resistively heated aluminum oxide crucibles, gold from a tungsten coil. The deposition rates were $\sim$0.2 nm/s for all materials, as monitored by a quartz crystal microbalance placed next to the substrate. For devices with Au as substrate, the freshly evaporated Au films (onto PEDOT/PSS) were sputtered with Ar ions. Au surfaces prepared under such conditions were confirmed to have a work function of 5.2 ± 0.2 eV by ultraviolet photoelectron spectroscopy. A shadow mask with arrays of holes was used to prepare the top Au contacts. $I(V)$ curves were measured *in situ* with a semiconductor parameter analyzer 4155B (Hewlett Packard). After bringing the samples to air, morphology analysis was performed with a multimode AFM (Digital Instruments) operated in tapping mode. The entire sample preparation and analysis was done at room temperature.

Two types of devices were prepared with each organic material: type 1 with the structure (bottom to top) ITO/(PEDOT/PSS)/organic(150 nm)/Au(45 nm), and type 2 with ITO/(PEDOT/PSS)/Au(80 nm)/organic(150 nm)/Au(45 nm). Type 2 devices were prepared with an intermediate PEDOT/PSS layer to assure identical ITO-surface smoothing. No additional energy barriers are introduced, as the conducting polythiophene layer forms Ohmic contacts to both ITO and Au. The $I(V)$ curves obtained *in situ* for devices made with α-NPD are shown in Fig. 1(a). The curves correspond to holes injected from the bottom PEDOT/PSS or top Au electrode in a type 1 device, or from the bottom Au or top Au electrode in a type 2 device. The key result is the difference of several orders of magnitude in hole current density (j) injected from PEDOT/PSS versus the Au electrodes. This difference can be directly linked to the 1 eV lowering of the hole barrier at the α-NPD interface with PEDOT/PSS as compared to Au.[9] The $I(V)$ curves for the α-NPD type 2, also shown in Fig. 1(a), show nearly identical hole injection from top and bottom Au contacts, demonstrating that there is no asymmetry in the $I(V)$ characteristics for contacts made by evaporation of Au onto the α-NPD film or by evaporation of the organic onto a Au surface. Note that these $I(V)$ curves are also nearly identical to those obtained for hole injection from the top Au contact in type 1 devices.

The $I(V)$ curves obtained for the similar series of devices made with pentacene are shown in Fig. 1(b). The hole current injected from PEDOT/PSS is higher by more than two orders of magnitude than that injected from the top Au contact in type 1 devices. As above, the more efficient hole injection from PEDOT/PSS can be attributed to the smaller injection barrier (by 0.6 eV).[9] However, in contrast to the α-NPD case, type 2 devices made from pentacene exhibit a pronounced asymmetry for hole injection from the bottom versus top Au contact. As seen in Fig. 1(b) above $\sim$4 V bias, j for hole injection from top Au electrodes is typically one order of magnitude higher than from bottom Au. Moreover, the current in either direction is 2–3 orders of magnitude smaller than for hole injection from the top Au contact in type 1 devices.

This behavior is, at first glance, inconsistent with a simple change in organic materials, i.e., pentacene versus α-NPD, and with the hole barriers reported above. However, it is explained by considering the different structural nature of the two materials: vacuum evaporated α-NPD films are amorphous, whereas pentacene films are (poly)crystalline. Figure 2 shows AFM micrographs of 150-nm-thick α-NPD films evaporated on PEDOT/PSS (left half) and on Au (right half). The height scale for both images is 10 nm. Although

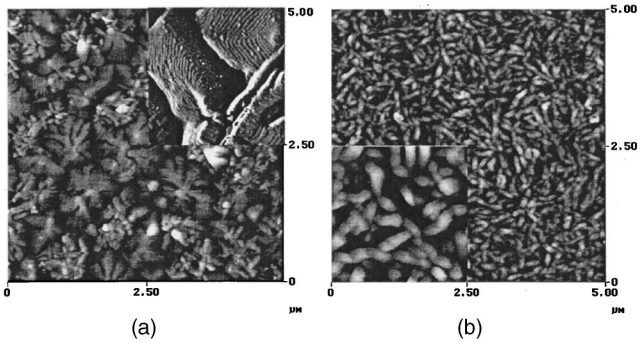

FIG. 3. (a) AFM micrograph of a 150-nm-thick pentacene film on PEDOT/PSS, height scale is 100 nm; the inset is a 600×600 nm^2 amplitude image. (b) AFM micrograph of a 150-nm-thick pentacene film on Au, height scale is 150 nm; the inset is a 1×1 μm^2 zoom, with a height scale of 100 nm.

the root-mean-square roughness of α-NPD is larger when deposited on Au (1.8 nm) than on PEDOT/PSS (1.1 nm), the maximum corrugation of <10 nm is still small for both films ($<7\%$ of the nominal film thickness). Thus, the $I(V)$ curves obtained for hole injection from Au are identical for type 1 and 2 devices [Fig. 1(a)].

AFM micrographs from a nominally 150-nm-thick pentacene film on PEDOT/PSS are shown in Fig. 3(a). The height scale in this case is 100 nm. The inset shows a close-up image of a 600×600 nm^2 area. The morphology is very similar to that of pentacene films grown on silicon oxide,[10,11] with nearly μm-size pyramid-like islands with monomolecular steps of ~1.4 nm. Additional AFM analysis of thinner pentacene films (nominal thickness: 6 nm) on PEDOT/PSS confirms that molecules in the first few monolayers are already aligned with their long axis almost perpendicular to the substrate surface (not shown here). On the thick films shown here, needle-like-shaped crystallites with random orientation can be observed in addition to the pyramidal islands. The corrugation of these pentacene films is almost as large as their nominal thickness. An entirely different morphology is observed for pentacene films deposited on Au [Fig. 3(b)]. Only needle-like crystallites ~100 nm wide, several hundred nm long, and with random orientation are observed. The surface corrugation is here again of the same order of magnitude as the nominal film thickness. We can assume that the preferred orientation of pentacene molecules in these needles is parallel to the Au surface, as the first few monolayers of pentacene have been shown to lie flat on Au.[12,13]

Consequently, the $I(V)$ curves of Fig. 1(b) are by no means representative for 150-nm-thick pentacene films, but are a superposition of curves from many locally different thicknesses across a device, the lower limit being probably as thin as a few monolayers. The much higher j for pentacene devices as compared to α-NPD devices can thus be due to (i) the presence of significantly thinner film areas and/or (ii) due to a higher charge carrier mobility in pentacene (up to three orders of magnitude).[11,14] Furthermore, the difference in morphology and preferred molecular orientation of pentacene on the two different substrates (PEDOT/PSS versus Au) leads to the discrepancies seen in the $I(V)$ characteristics for hole injection from Au in types 1 and 2 devices [Fig. 1(b)]. However, the simultaneous variation of typical crystallite size, density of grain boundaries, fraction of thinner film areas, and preferred molecular orientation when switching from PEDOT/PSS to Au as substrate makes it virtually impossible to differentiate between these individual parameters. Moreover, the offset in j for hole injection from the top versus the bottom Au contact (for type 2) may have its origin in a still different preferred molecular orientation for molecules close to the Au substrate and those pentacene molecules on top of the organic film. Consequently, one has to take great care when trying to evaluate $I(V)$ curves of devices comprised of crystalline organic solids; especially when the influence of film thickness or different substrate materials is to be studied.

We have shown that hole injection from PEDOT/PSS contacts into organic materials (α-NPD and pentacene) is much more efficient than from Au contacts, albeit the similar work function of both electrode surfaces. This is due to the significantly lower hole injection barriers between the molecular materials and the conducting polymer. Furthermore, it was demonstrated that the interpretation of $I(V)$ characteristics becomes impractical if the exact sample morphology is unknown. This is most important for thin film device studies performed on crystalline organic materials, such as pentacene.

Support by the NSF (DMR-0097133) and the New Jersey Center for Organic OptoElectronics is gratefully acknowledged.

[1] H. Ishii and K. Seki, IEEE Trans. Electron Devices **44**, 1295 (1997).
[2] I. G. Hill, A. Rajagopal, A. Kahn, and Y. Hu, Appl. Phys. Lett. **73**, 662 (1998).
[3] I. G. Hill, A. J. Makinen, and Z. H. Kafafi, Appl. Phys. Lett. **77**, 1825 (2000).
[4] *Conjugated Polymer and Molecular Interfaces: Science and Technology for Photonic and Optoelectronic Applications*; Vol., edited by W. R. Salaneck, K. Seki, A. Kahn, and J.-J. Pireaux (Marcel Dekker, New York, 2001).
[5] C. Shen, A. Kahn, and J. Schwartz, J. Appl. Phys. **89**, 449 (2001).
[6] H. Ishii, K. Sugiyama, E. Ito, and K. Seki, Adv. Mater. **11**, 605 (1999).
[7] S. A. Carter, M. Angelopoulos, S. Karg, P. J. Brock, and J. C. Scott, Appl. Phys. Lett. **70**, 2067 (1997).
[8] A. Elschner, F. Bruder, H. W. Heuer, F. Jonas, A. Karbach, S. Kirchmeyer, and S. Thurm, Synth. Met. **111**, 139 (2000).
[9] N. Koch, J. Ghijsen, A. Elschner, R. L. Johnson, J.-J. Pireaux, J. Schwartz, and A. Kahn, Appl. Phys. Lett. **82**, 70 (2003)
[10] D. J. Gundlach, Y. Y. Lin, T. N. Jackson, S. F. Nelson, and D. G. Schlom, IEEE Electron Device Lett. **18**, 87 (1997).
[11] C. D. Dimitrakopoulos and P. R. L. Malenfant, Adv. Mater. **14**, 99 (2002).
[12] P. G. Schroeder, C. B. France, J. B. Park, and B. A. Parkinson, J. Appl. Phys. **91**, 3010 (2002).
[13] C. B. France, P. G. Schroeder, and B. A. Parkinson, Nano Lett. **2**, 693 (2002).
[14] S. Naka, H. Okada, H. Onnagawa, Y. Yamaguchi, and T. Tsutsui, Synth. Met. **111**, 331 (2000).